

# PROCEEDINGS OF SPIE

[SPIDigitalLibrary.org/conference-proceedings-of-spie](https://spiedigitallibrary.org/conference-proceedings-of-spie)

## The Atacama cosmology telescope project

Fowler, Joseph

Joseph W. Fowler, "The Atacama cosmology telescope project," Proc. SPIE 5498, Millimeter and Submillimeter Detectors for Astronomy II, (8 October 2004); doi: 10.1117/12.553054

**SPIE.**

Event: SPIE Astronomical Telescopes + Instrumentation, 2004, Glasgow, United Kingdom

# The Atacama Cosmology Telescope Project

Joseph W. Fowler<sup>a</sup>, for the ACT Collaboration.

<sup>a</sup>Princeton University, Department of Physics, Jadwin Hall, Washington Road, Princeton,  
New Jersey 08544, USA;

## ABSTRACT

The Atacama Cosmology Telescope (ACT) is a new, 6-meter aperture, millimeter-wave telescope that will be located at an altitude of 5200 meters in the Chilean Andes. ACT will be fielded with the Millimeter Bolometric Array Camera (MBAC). The MBAC will incorporate arrays of “pop-up” bolometers using multiplexed Transition Edge Sensors (TES), developed at NASA/GSFC and NIST. The camera will consist of three arrays for multi-frequency ground-based millimeter observations near 150, 220 and 270 GHz. The goal is to map the cosmic microwave background and discover Sunyaev-Zel’dovich clusters. Associated follow-up observations of the clusters will be taken at optical and X-ray wavelengths.

**Keywords:** CMB, bolometers, detectors, arrays, TES

## 1. INTRODUCTION

Exciting recent discoveries in observational and theoretical cosmology have given us a glimpse of new fundamental physics. Our conception of the contents and fate of the universe is clearer and dramatically different than it was just a decade ago. We now believe the Universe is geometrically flat and comprised of 4% baryons, 23% dark matter, and 73% a new form of dark energy.<sup>1,2</sup>

A revolution in detector technology, namely thousand-element CCD-like bolometric arrays, has opened the door to new discoveries about the physical universe. The Millimeter Bolometric Array Camera (MBAC) will use three 1000-element detector arrays at 150, 220, and 270 GHz. The MBAC will be coupled to a 6-meter telescope. Observations with this instrument can map out the formation of cosmic structure from the high-redshift ( $z \sim 1100$ ) linear regime through the low-redshift ( $z \geq 5$ ) non-linear regime when structures form. Optical spectroscopy with 10-meter class telescopes and measurements with modern X-ray satellites will enable the determination of the redshifts and masses of hundreds of galaxy clusters, the latest stage of cosmic evolution. The goals of the experiment are to:

- Map the CMB temperature anisotropy over  $100 \text{ deg}^2$ , beyond the resolution limits of the WMAP and Planck satellites, with a target error of  $2 \mu\text{K}/\text{pixel}$  for  $1.7' \times 1.7'$  pixels. The primary anisotropy constrains the fundamental physics of the infant universe and provides the initial conditions for structure formation; the secondary anisotropies reflect the emergence of structure.
- Find all galaxy clusters with  $M > 4 \times 10^{14} M_{\odot}$  in the CMB map region through the Sunyaev-Zel’dovich effect and determine the spectroscopic redshift of over 400 of them. The masses of these clusters will be determined with a combination of X-ray observations and with galaxy velocity dispersions.
- Combine the CMB and cluster measurements to limit or determine the mass of the neutrino to  $\pm 0.1 \text{ eV}$ . The current cosmological limit on the sum of the light neutrino masses is  $0.7 \text{ eV}$ .<sup>3</sup>
- Find the equation of state,  $w = p/\rho$ , of the “quintessence” or “dark energy” to  $\pm 0.1$  through the CMB/cluster combination.
- Measure the amplitude of gravitational lensing of the CMB to probe the unbiased matter power spectrum. This technique is independent of and complementary to lower redshift galaxy surveys (which involve luminosity bias), though it requires unprecedented control of systematic errors.
- Detect reionization of the universe from the formation of the first stars at  $z \sim 10$  through the Ostriker-Vishniac effect in the CMB.

## 2. THE MILLIMETER BOLOMETRIC ARRAY CAMERA

Over the past seven years, members of the ACT team at GSFC and NIST have developed a new infrared technology comprised of CCD-like arrays of nearly touching bolometers (Figure 1). Recent bolometric cameras use  $\approx 100$  individual detectors, each with its own electronics and optics.<sup>4,5</sup> The new generation will employ hundreds to thousands of close-packed detectors in a multiplexed readout scheme. This new format opens frontiers in ground-based millimeter-wave image synthesis, control of systematic errors, and observing strategies.

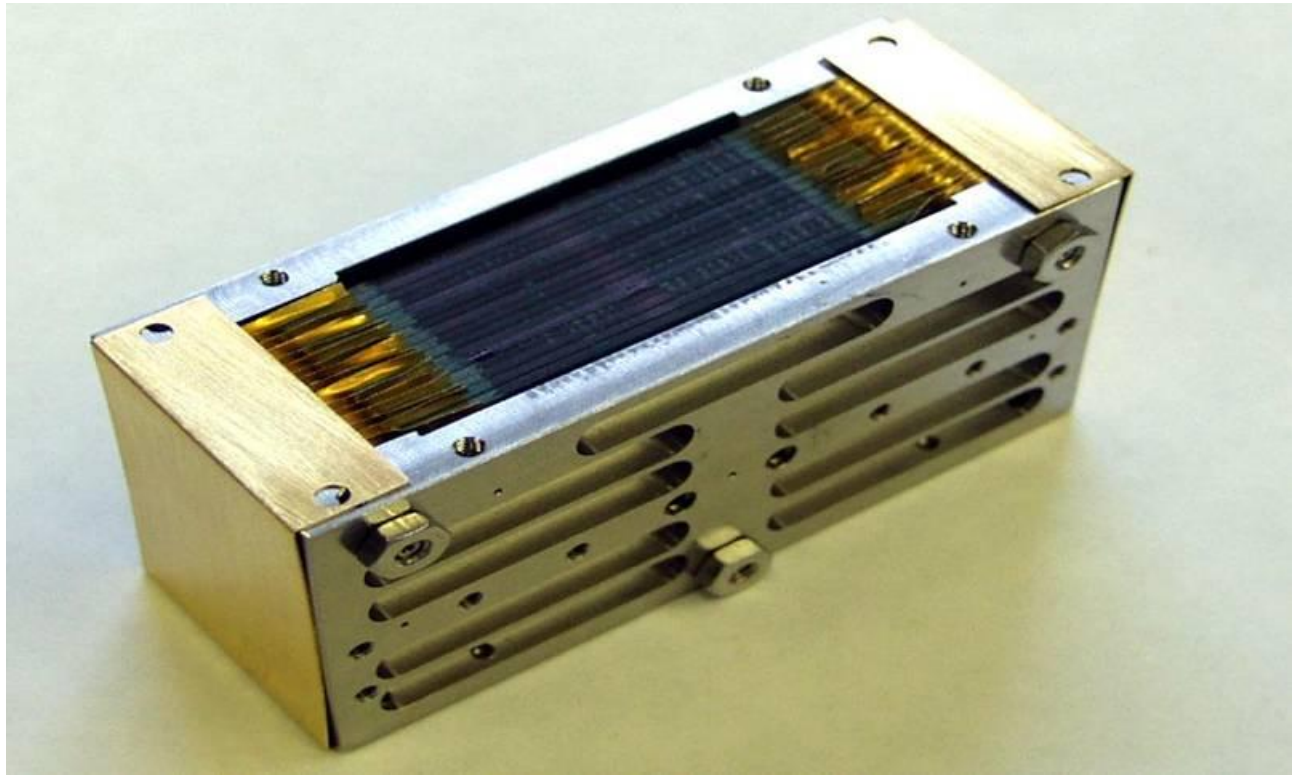


**Figure 1.** Photograph of the SAFIRE  $16 \times 32$  pop-up array. The MBAC arrays will use the same detector technology. Each row of 32 is folded and processed as a unit; each element is  $1 \text{ mm}^2$ . The rows are stacked together to form a two dimensional array. The multiplexing/readout electronics are designed to fit in the space directly under the rows of detectors. Image courtesy of SAFIRE instrument team ([http://sofia.arc.nasa.gov/Science/instruments/instruments\\_safire.html](http://sofia.arc.nasa.gov/Science/instruments/instruments_safire.html)).

The Millimeter Bolometric Array Camera (MBAC) plans use three separate  $32 \times 32$  arrays of  $1 \text{ mm}^2$  transition edge sensors (TES) detectors<sup>6,7</sup> on pop-up arrays (Figure 2). These detector arrays have a number of distinct advantages over traditional bolometers. Each array is read out with a Superconducting Quantum Interference Device (SQUID) multiplexer (MUX)<sup>8</sup> to minimize the number of connections to the dewars. Also, the elements are close-packed so that the sky is continuously and fully sampled without gaps.

Similar GSFC arrays, with  $N_{det} \approx 100 - 10,000$ , are in the development and deployment stages for use at wavelengths ranging from  $\lambda = 145$  to  $850 \mu\text{m}$  (Table 2.1). Our baseline design is similar to a system already used to observe the sky at  $350 \mu\text{m}$  and  $450 \mu\text{m}$  with the FIBRE spectrometer.<sup>9</sup> We would be the first to deploy these arrays at long wavelengths ( $\lambda > 1110 \mu\text{m}$  for ACT). Our goal is to bring the power of this new technology to bear on frontier questions in cosmology.

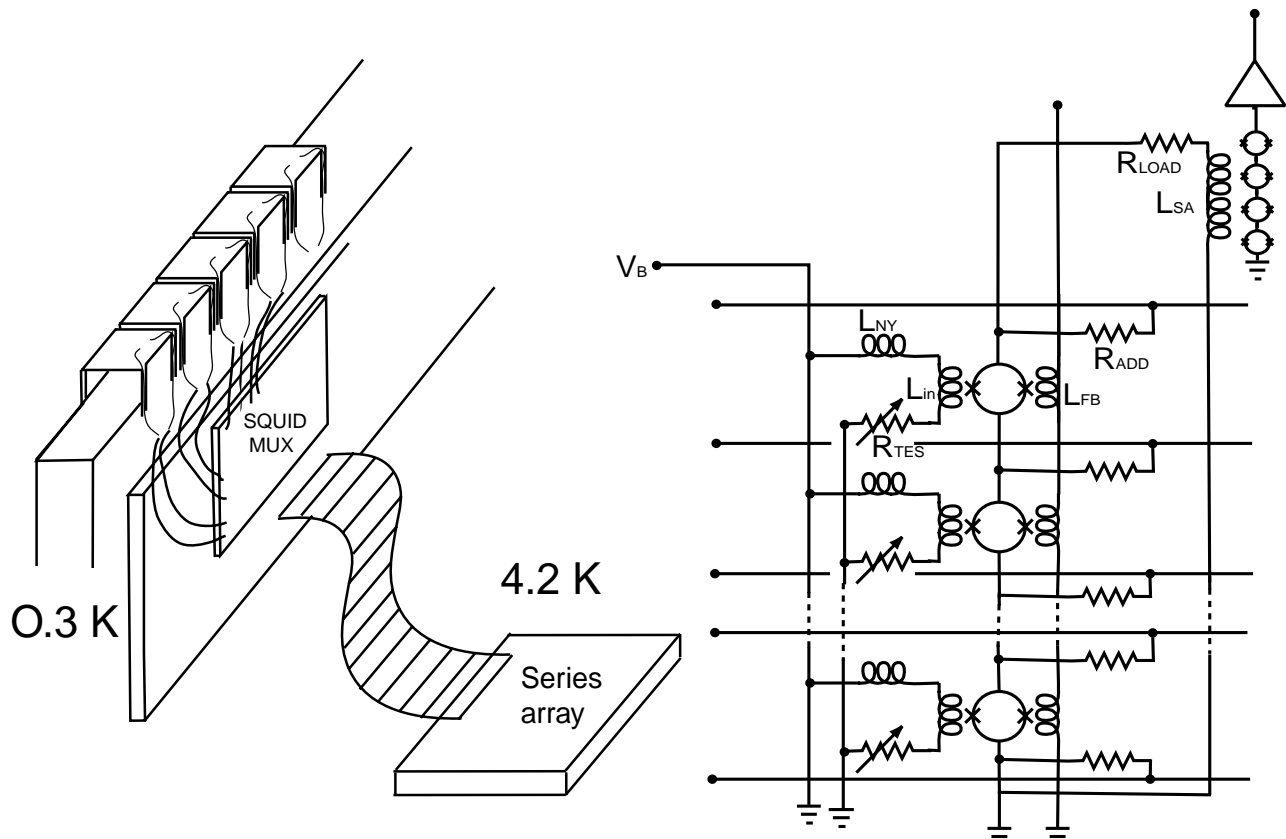


**Figure 2.** *Left:* Schematic of five Goddard TES detectors on the silicon pop-up structure. Leads from the TES go to the NIST SQUID multiplexer chip at 270 mK. The dissipation for the  $32 \times 32$  array is  $\approx 0.5 \mu\text{W}$ . From the MUX, superconducting niobium lines take the signal to the SQUID series array, which can be located 30 cm away. Cryogenic transmission line runs from the series array output to warm electronics. Magnetic shielding surrounds all SQUIDS. From one  $32 \times 32$  array, the total number of wires is 228, compared to more than 2000 without multiplexing. *Right:* Electronic schematic for the TES MUX array. The series array is in the upper right hand corner.

## 2.1. Multiplexed Transition Edge Sensor Arrays

The MBAC is designed to be as simple as possible. In the baseline design, it uses three independent arrays, each observing the sky through separate band-defining filters. Figure 3 shows the band positions superimposed on a plot of the atmosphere at the Chilean site. Also shown on the plot are the signatures of extragalactic point sources, the CMB anisotropy, and the Sunyaev-Zel'dovich effect. The results of an eigenmode analysis of the three bands shows what is evident to the eye: fluctuations in any of these three sources have a unique signature. The 225 GHz band is principally sensitive to CMB fluctuations rather than clusters.

The base temperature of the arrays will be maintained near 270 mK using a combination of 4 K and 60 K pulse tube refrigeration and pumped  $^3\text{He}$  systems. There will be no consumable cryogenes. TES arrays are particularly well suited to operation with mechanical coolers. The intrinsic device impedance is  $\approx 0.3 \Omega$ , and consequently there is minimal microphonic sensitivity.

The coupling optics between the MBAC and the telescope will include a cryogenic pupil (“cold Lyot stop”) to block stray light from loading the detectors and to ensure that the detectors are imaged onto the primary mirror. Such an approach has been used successfully on previous mm-wave and IR experiments. The telescope will feed the MBAC at a focal ratio of  $F \approx 3$ . In the cryostat, after the filtering and IR blocking, cold optics will reduce the focal ratio to  $F \approx 1$  to feed the arrays.

The NIST Electromagnetic Technology Division, working closely with the GSFC group, has developed all the equipment required to interface a  $32 \times 32$  array with SQUID multiplexers. Items built and tested include

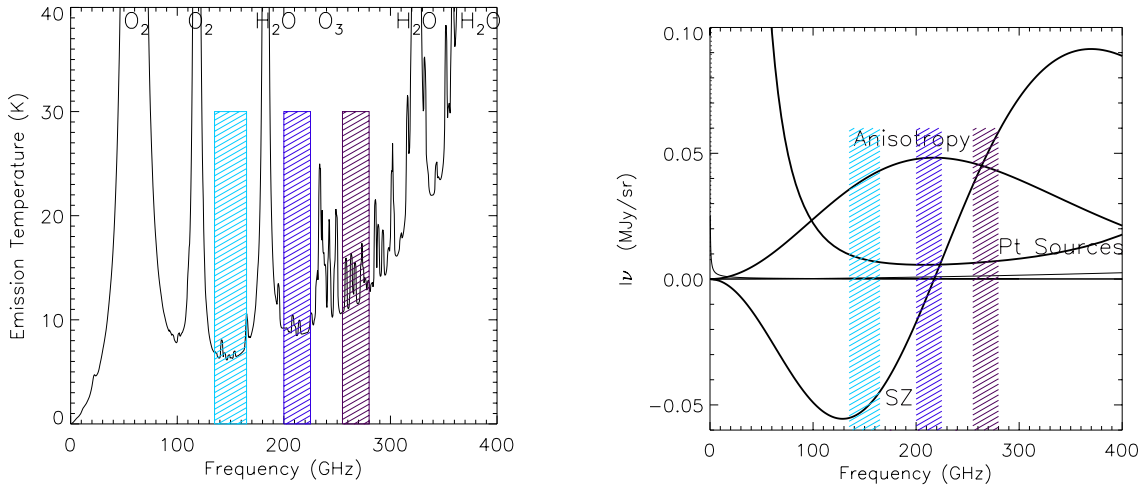


**Figure 3.** *Left:* Atmospheric emission on Cerro Toco. The zenith optical depth shown is 0.04, which is achieved > 35% of the time in Austral winter and spring, and  $\approx 25\%$  of the time in summer. *Right:* The fluctuation spectrum of the mm-wave sky with our spectral bands. The anisotropy is given as  $(\partial B_\nu / \partial T) \delta T$  with  $\delta T = 100 \mu\text{K}$  and we use a Compton  $y = 5 \times 10^{-5}$  for the S-Z effect, typical for a  $z = 0.5$  cluster. The central band will not see any SZ contribution, only CMB and point sources.<sup>10,11</sup> The fluctuation levels for diffuse free-free, synchrotron, and dust emission are for a Galactic latitude of  $b = 20^\circ$  and  $l = 1000$ .<sup>10,12</sup> In our  $l$ -range they are negligible, as shown in the plot by the small line near zero. The CMB anisotropy, point sources, and SZ effects are separable by their frequency signatures. Note that the point source contamination is minimal near our frequencies and will be a larger issue for measurements at lower frequencies.

the SQUID multiplexer chips, fabricated using NIST facilities for niobium trilayer processing. These chips will be built as  $1 \times 32$  units. They operate at 0.3 K and dissipate only  $\approx 10$  nW.

Experiment	Wavelength	Receiver	Size	Site	Cryo
FIBRE	350-850 $\mu\text{m}$	TFP	1 $\times$ 16	CSO	<sup>3</sup> He
HAWC	60-210 $\mu\text{m}$	TFP	12 $\times$ 32	SOFIA	ADR
SHARC-II	350/450 $\mu\text{m}$	Camera	12 $\times$ 24	CSO	<sup>3</sup> He
SIFI	350 $\mu\text{m}$	IFP	4 $\times$ 32	JCMT	<sup>3</sup> He
SAFIRE	350 $\mu\text{m}$	IFP	12 $\times$ 24	SOFIA	<sup>3</sup> He
SCUBA-2	450 $\mu\text{m}$	Camera	160 $\times$ 160	JCMT	Dil
	850 $\mu\text{m}$	Camera	80 $\times$ 80	JCMT	Dil
<b>MBAC</b>	<b>2070 <math>\mu\text{m}</math></b>	<b>Camera</b>	<b>32<math>\times</math>32</b>	<b>ACT</b>	<b><sup>3</sup>He</b>
	<b>1330 <math>\mu\text{m}</math></b>	<b>Camera</b>	<b>32<math>\times</math>32</b>	<b>ACT</b>	<b><sup>3</sup>He</b>
	<b>1130 <math>\mu\text{m}</math></b>	<b>Camera</b>	<b>32<math>\times</math>32</b>	<b>ACT</b>	<b><sup>3</sup>He</b>

**Table 1.** A sample of array detectors and receivers. TFP = Tunable Fabry-Perot. IFP = Imaging Fabry-Perot. ADR=Adiabatic demagnetization refrigerator,  $T < 100$  mK. <sup>3</sup>He = pumped <sup>3</sup>He system,  $T \approx 300$  mK. Dil = dilution refrigerator,  $T < 100$  mK.

## 2.2. Target Camera specifications

We have modeled the detectors, the telescope, the site, and cryogenics to ensure that such a system can be built without a burdensome development program. Our nominal configuration, given in Table 2, has the arrays fed at  $F = 1$  in all bands so that each array instantaneously and simultaneously images approximately  $20' \times 20'$  of sky. The arrays are physically identical so the pixel spacing ranges from  $0.5F\lambda$  to  $0.9F\lambda$  for the long to short

wavelength bands respectively. We are currently optimizing this design to extract the cosmological signal in the presence of the atmosphere. A balance must be found, because a large field of view increases mapping speed, but it also has reduced optical efficiency and loses sensitivity to the highest spatial frequencies.

Quantity	Band 1	Band 2	Band 3	Comments
Frequency (GHz)	145	225	265	Atmospheric windows
Bandwidth (GHz)	30	25	30	
$N_{det}$	1024	1024	1024	
$N_{res}$	169	400	576	Resolution elements/array
Resolution	1.7'	1.1'	0.9'	Diffraction limited
$\eta$	6%	10%	12%	Coupling, optical, pixel efficiency
$T_{atm}$ (K)	7	14	20	Atmospheric temperature
$\epsilon_{optics} T_{optics}$ (K)	15	23	23	Effective optics temperature
$P_{det}$ (pW)	2	4	8	Incident power on detector
$NEP$ (W sec <sup>1/2</sup> )	$2 \times 10^{-17}$	$3 \times 10^{-17}$	$4 \times 10^{-17}$	Total (detector and photon shot noise)
$\delta T_{CMB}/\delta T_{RJ}$	1.7	3.1	4.7	CMB-RJ Conversion
$S$ ( $\mu$ K sec <sup>1/2</sup> )	300	500	700	Target CMB Sensitivity/detector

**Table 2.** Target characteristics of the MBAC.

The close packed TES arrays, with their full sampling of the field, fast response, sensitivity, and stability, open up new possibilities in image synthesis and observing strategies. With the high level of redundancy, one may scan the array over the sky at rates of  $\approx 1^\circ/\text{sec}$  and solve for the celestial component in the presence of atmospheric and instrumental fluctuations. Each sky pixel will be observed with detectors on six time scales:  $\tau_{pix\ transit} \approx 0.02\text{ s}$ ,  $\tau_{array\ transit} \approx 0.4\text{ s}$ ,  $\tau_{sweep} \approx 3\text{ s}$ ,  $\tau_{pix\ drift} \approx 9\text{ s}$ ,  $\tau_{array\ drift} \approx 3\text{ min}$ , and  $\tau_{sky} \approx 7\text{ hrs}$ .<sup>\*</sup> In addition, each sky pixel will be scanned in a cross-linked pattern by observing it both in the southwest and southeast. This highly interlocking set of constraints provides a strong spatiotemporal filter that will control systematic errors to very low levels.

Traditional focal plane arrays are sparsely sampled and employ a variety of techniques to fully sample the sky while simultaneously minimizing the atmospheric signal. The groundbreaking SCUBA instrument moved a chopper in a jiggle pattern at 7.8 Hz to measure multiple positions on the sky and then reconstruct an image of blank sky.<sup>4</sup> Bolocam uses the on-axis CSO with a drift scan and differencing in software, combined with telescope repositioning, to produce an image.<sup>13</sup> The MAT/TOCO<sup>14</sup> and ACBAR<sup>15</sup> experiments scan the arrays across the sky at  $\approx 3\text{ Hz}$  with a chopping optic. We believe that new methods will be needed to take advantage of the extraordinary sensitivity of TES arrays.

Our whole telescope will move and scan the arrays across the sky, with no chopping optical components, so that the transit time for a point source is  $\tau_{array\ transit} \approx 0.4\text{ s} < \tau_{knee}$ . With our nominal design, this puts the sample frequency ( $f_{samp} = 2.5/\tau_{pixel\ transit}$ ) for a single detector at 110 Hz: the need for fast detectors is evident. The atmospheric contribution also has an approximate  $1/f$  spectrum and is separable from the celestial contribution because wind drives it by the telescope at speeds of order  $0.5^\circ/\text{s}$ . However, this contribution is calculated to be negligible at most spatial frequencies. Because we fully sample the sky and observe each pixel multiple times with multiple detectors, we aim to solve for the true sky signal in the presence of  $1/f$  variations and atmospheric fluctuations. We will use algorithms based on the work of Dave Cottingham,<sup>16</sup> for the analysis of FIRS.<sup>17</sup> In essence, the number of degrees of freedom needed for the atmospheric/detector solution is far smaller than the number of spatial pixels. This is different from the traditional ‘‘averaging down’’ of the atmosphere. An additional benefit of a fully sampled array is that cosmic rays are easily identified.<sup>18</sup> A millimeter-wave camera of this sort is approaching the functionality of an infrared CCD camera.<sup>19</sup>

<sup>\*</sup>The time scales are set by how fast the sky moves across the pixels and across the array, both in the telescope sweep direction and in the sky drift direction.

### 3. THE ATACAMA COSMOLOGY TELESCOPE

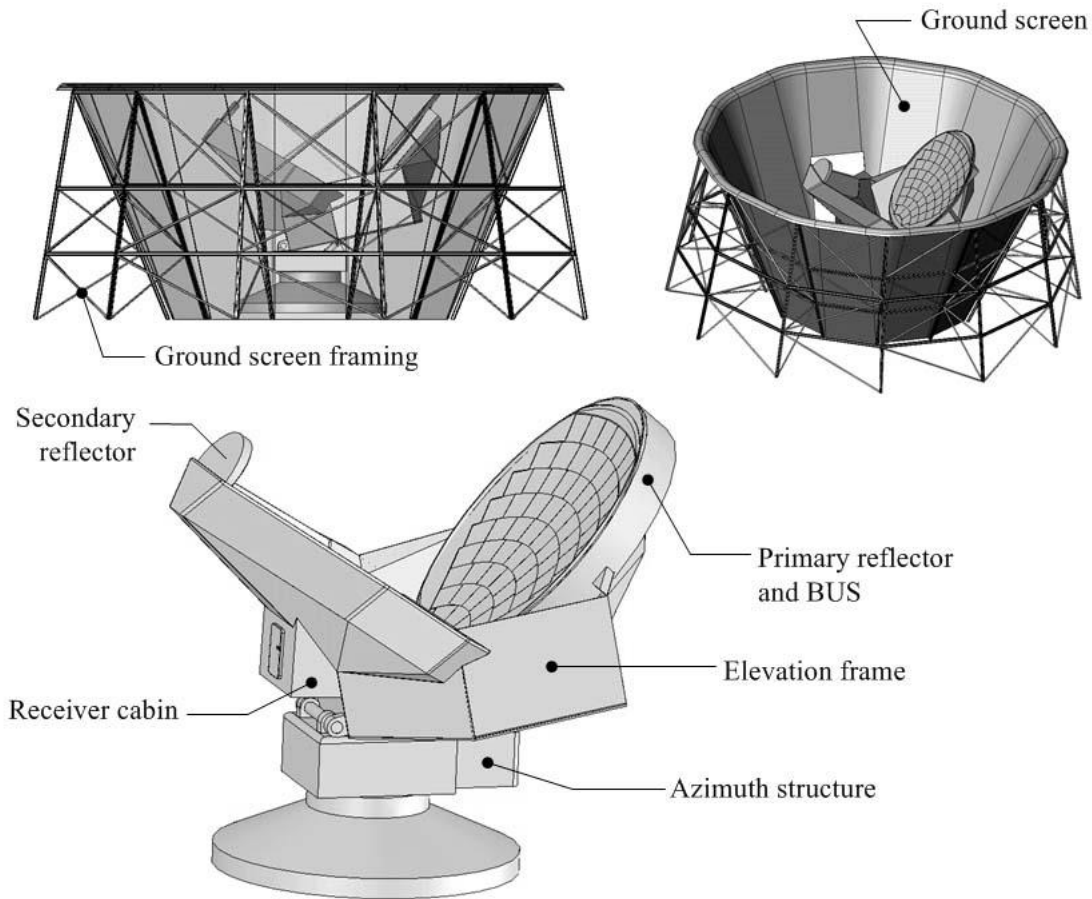


**Figure 4.** Preliminary design drawing of the Atacama Cosmology Telescope. AMEX Dynamic Structures Ltd. will build the telescope.

The need to control systematic errors to the level of  $\mu\text{K}$  drives most aspects of the telescope design. The Atacama Cosmology Telescope will be an off-axis Gregorian, with a primary diameter of 6 meters. The telescope will be manufactured by AMEC Dynamic Structures, Ltd. of Port Coquitlam, British Columbia. The diffraction-limited resolution will be approximately 1.7 arcminutes at 150 GHz and 1 arcminute at 270 GHz. Reimaging optics, dichroic beamsplitters, low-pass and bandpass filters, and a cold Lyot stop will be contained inside a large cryostat. The reimaging optics will likely require one or more cold silicon lenses, and we are currently refining a technique for reducing their reflectivity, which would otherwise cause a 30% power loss per surface.

The telescope profile is as low as possible, and ground shields will surround the system to reduce ground pickup and to place beam spillover onto the sky. A “guard ring” will surround the primary mirror in an approximate and inexpensive extension of the primary mirror shape, also to reflect spillover to the sky.

The ACT primary and secondary mirrors will be designed to meet the Dragone “on-axis equivalent paraboloid” condition, keeping cross-polarization as low as possible.<sup>20–22</sup> The initial observations with MBAC will measure only the sky temperature, but the polarization-preserving Gregorian paves the way for polarimetric measurements in the future.

The entire telescope will sit on a large bearing and scan continuously back and forth in azimuth. In this way, a constant-elevation scan can be executed without any reflecting or diffracting surface moving with respect to the receiver. This construction challenge is part of the overriding strategy of minimizing scan-synchronized offset. The current CMB observing plan calls for operating at a fixed elevation of  $45^\circ$ . The observations will be made at a small range of declinations near  $\delta \sim 60^\circ$  South. By observing the same ring of sky both to the east and west of the south celestial pole, ACT will make highly cross-linked maps of the survey area. Such maps minimize the striping that results from low-frequency detector gain variations and atmospheric structure. The effective temperature of the atmosphere varies by thousands of microkelvin per arcminute. Taking observations at constant elevation therefore has the advantage of keeping the atmospheric slant depth constant, again minimizing the artificial stripes in the maps. The telescope will also have the ability to move through a limited elevation range for pointed observations (*e.g.*, of planets) and for vertical nodding of the array, should it prove necessary.

The telescope will be deployed on Cerro Toco in the Atacama Desert region of the Chilean Andes. The Toco site has an altitude of 5100 meters and is within ten kilometers of the ALMA,<sup>23</sup> APEX,<sup>24</sup> and CBI<sup>25</sup> experiments. Its location at  $23^\circ$  south latitude gives us access to more than 60% of the sky. The large overlap with both northern and southern hemisphere telescopes is important to our plans for follow-up optical observations to determine cluster redshifts.

Because of the ALMA project, the NRAO has been characterizing the atmosphere and climate in the area of the Llano Chajnator for several years. Opacities at 225 GHz over the last few years are cataloged at the ALMA web site <http://www.alma.nrao.edu/>. The atmosphere in the high Atacama is comparable to that of the South Pole, where other large CMB projects are under way. The MAT/TOCO experiment found the median sky temperature above Cerro Toco to be 9 K at 150 GHz during the period September through December of 1998 and 1999.<sup>14</sup> Using the approach of Lay and Halverson,<sup>26</sup> we expect that atmospheric fluctuation power will exceed receiver noise only for scales larger than  $\sim 30$  arcminutes. Additionally, some of the large-scale atmospheric structure can be removed from the maps by taking advantage of its long coherence time and the dense sampling of the ACT focal plane. ACT will operate only during that half of the year when conditions in the Atacama are most favorable for millimeter-wave observations.

The ACT map will cover approximately 200 square degrees, in a region not yet exactly specified. We expect that half of the survey region will be suitable for cosmological analysis, while the other half will contain the galactic plane.

#### 4. ASSOCIATED GALAXY CLUSTER SURVEYS

ACT will identify on the order of one thousand galaxy clusters in the survey region (depending on cosmology). The limiting mass will be a few times  $10^{14} M_\odot$ , almost independent of redshift. To derive all possible science from the cluster catalog requires knowledge of cluster redshifts. Our optical follow-up survey will use the Prime Focus Imaging Spectrograph on the 11-meter Southern African Large Telescope (SALT, <http://www.salt.ac.za/>), which is currently being built in the Karoo Desert of South Africa. The survey goal is to obtain cluster redshifts and velocity dispersions of cluster member galaxies for 400 clusters over two years. Rutgers, a 10% partner in SALT construction, has committed 10 nights of observing per year to ACT follow-up. Further spectroscopic redshifts, as well as photometric ones, will be measured by our Chilean collaborators using various telescopes in Chile and by our South African collaborators using other SALT instruments.

We will also propose X-ray imaging of a subset of the ACT clusters, using the Chandra and XMM satellites. The X-ray images provide information about the cluster masses, densities, and temperatures. The techniques for converting X-ray flux or temperatures to cluster masses are well-known,<sup>27,28</sup> if subject to systematic errors owing to cluster structure and non-isothermality. By studying cluster masses in as many ways as possible (SZ signal, galaxy velocity dispersion, and X-ray imaging), we expect to characterize the mass cutoff of the ACT cluster sample. Understanding this cutoff is an important in inferring cosmological parameters from the cluster counts.<sup>29</sup>

## 5. ACT CURRENT STATUS

The ACT project was funded and officially started in January 2004. Prototype work was already well underway by that time, particularly on the TES bolometers, the multiplexed readout, and cryogenic and optical design. The telescope vendor has been selected, and ACT is scheduled for delivery to the site in mid-2006. Full three-color observations are to start one year later. The SALT telescope and prime focus spectrograph are on schedule and budget to achieve first light in early 2005.

New detector technologies, combined with the field's growing experience with making low-systematics measurements, will soon lead to microwave background maps of unprecedented sensitivity. We anticipate that the Atacama Cosmology Telescope will contribute a large, high-fidelity map at arcminute scales, giving us a number of exciting and new cosmological probes.

## ACKNOWLEDGMENTS

ACT is a large international collaboration and builds on technologies and techniques developed at individual institutes over many years. The project website can be found at <http://www.hep.upenn.edu/act/>. The ACT collaboration includes Cardiff University, CUNY York College, Columbia University, Haverford College, INAOE (México), NASA Goddard Space Flight Center, National Institute of Standards and Technology at Boulder, Pontificia Universidad Católica de Chile, Princeton University, Rutgers University, University of British Columbia, University of KwaZulu-Natal (South Africa), University of Massachusetts, University of Pennsylvania, and University of Toronto. The ACT guiding board is composed of Mark Devlin, Kent Irwin, Arthur Kosowsky, Harvey Moseley, Lyman Page (PI), Hernan Quintana, David Spergel, and Suzanne Staggs. Initial development was supported by NSF awards PHY00-99493 to Princeton and AST97-32960 to the University of Pennsylvania. The NSF supports ACT under award AST-0140585.

## REFERENCES

1. W. L. Freedman and M. S. Turner, "Measuring and understanding the universe," *Rev. Mod. Phys.* **75**, pp. 1433–1447, 2003.
2. J. P. Ostriker and P. J. Steinhardt, "New light on dark matter," *Science* **300**, pp. 1909–1913, 2003.
3. D. N. Spergel, L. Verde, H. V. Peiris, E. Komatsu, M. R.olta, C. L. Bennett, M. Halpern, G. Hinshaw, N. Jarosik, A. Kogut, M. Limon, S. S. Meyer, L. Page, G. S. Tucker, J. L. Weiland, E. Wollack, and E. L. Wright, "First-Year Wilkinson Microwave Anisotropy Probe (WMAP) Observations: Determination of Cosmological Parameters," *ApJS* **148**, pp. 175–194, Sept. 2003.
4. W. S. Holland, E. I. Robson, W. K. Gear, C. R. Cunningham, J. F. Lightfoot, T. Jenness, R. J. Ivison, J. A. Stevens, P. A. R. Ade, M. J. Griffin, W. D. Duncan, J. A. Murphy, and D. A. Naylor, "SCUBA: a common-user submillimetre camera operating on the James Clerk Maxwell Telescope," *MNRAS* **303**, pp. 659–672, Mar. 1999.
5. C. L. Carilli *et al.*, "Wide field imaging at 250 ghz," in *Deep Millimeter Surveys: Implications for Galaxy Formation and Evolution*, 2000.
6. A. Lee, P. Richards, S. Nam, B. Cabrera, and K. Irwin, "A superconducting bolometer with strong electrothermal feedback," *Appl Phys Lett* **69**, pp. 1801–1803, 1996.
7. K. D. Irwin, G. C. Hilton, D. A. Wollman, , and J. M. Martinis, "X-ray detection using a superconducting transition-edge sensor microcalorimeter with electrothermal feedback," *Appl Phys Lett* **69**, pp. 1945–1947, 1996.
8. J. A. Chervenak, K. D. Irwin, E. N. Grossman, J. M. Martinis, C. D. Reintsema, and M. E. Huber, "Superconducting multiplexer for arrays of transition edge sensors," *Appl Phys Lett* **74**, pp. 4043–4045, 1999.
9. D. J. Benford *et al.*, "First astronomical use of multiplexed transition edge bolometers," in *Ninth Workshop on Low Temperature Detectors, AIP Proceedings*, 2001.

10. M. Tegmark and et al., "Overview of Foregrounds and their Impact," in *ASP Conf. Ser. 181: Microwave Foregrounds*, pp. 3–+, 1999.
11. L. Toffolatti, F. Argueso Gomez, G. de Zotti, P. Mazzei, A. Franceschini, L. Danese, and C. Burigana, "Extragalactic source counts and contributions to the anisotropies of the cosmic microwave background: predictions for the Planck Surveyor mission," *MNRAS* **297**, pp. 117–127, June 1998.
12. A. de Oliveira-Costa, M. Tegmark, D. P. Finkbeiner, R. D. Davies, C. M. Gutierrez, L. M. Haffner, A. W. Jones, A. N. Lasenby, R. Rebolo, R. J. Reynolds, S. L. Tufte, and R. A. Watson, "A New Spin on Galactic Dust," *ApJ* **567**, pp. 363–369, Mar. 2002.
13. J. Glenn, P. A. R. Ade, M. Amarie, J. J. Bock, S. F. Edgington, A. Goldin, S. Golwala, D. Haig, A. E. Lange, G. Laurent, P. D. Mauskopf, M. Yun, and H. Nguyen, "Current status of Bolocam: a large-format millimeter-wave bolometer camera," in *Millimeter and Submillimeter Detectors for Astronomy. Edited by Phillips, Thomas G.; Zmuidzinas, Jonas. Proceedings of the SPIE, Volume 4855, pp. 30-40 (2003).*, pp. 30–40, Feb. 2003.
14. A. Miller, J. Beach, S. Bradley, R. Caldwell, H. Chapman, M. J. Devlin, W. B. Dorwart, T. Herbig, D. Jones, G. Monnelly, C. B. Netterfield, M. Nolta, L. A. Page, J. Puchalla, T. Robertson, E. Torbet, H. T. Tran, and W. E. Vinje, "The QMAP and MAT/TOCO Experiments for Measuring Anisotropy in the Cosmic Microwave Background," *ApJS* **140**, pp. 115–141, June 2002.
15. M. C. Runyan, P. A. R. Ade, R. S. Bhatia, J. J. Bock, M. D. Daub, J. H. Goldstein, C. V. Haynes, W. L. Holzapfel, C. L. Kuo, A. E. Lange, J. Leong, M. Lueker, M. Newcomb, J. B. Peterson, C. Reichardt, J. Ruhl, G. Sirbi, E. Torbet, C. Tucker, A. D. Turner, and D. Woolsey, "ACBAR: The Arcminute Cosmology Bolometer Array Receiver," *ApJS* **149**, pp. 265–287, Dec. 2003.
16. D. A. Cottingham, "A sky temperature survey at 19.2 GHz using a balloon borne Dicke radiometer for anisotropy tests of the cosmic microwave background," *Princeton University Ph.D. Thesis*, 1987.
17. K. Ganga, E. Cheng, S. Meyer, and L. Page, "Cross-correlation between the 170 GHz survey map and the COBE differential microwave radiometer first-year maps," *ApJ* **410**, pp. L57–L60, June 1993.
18. D. J. Fixsen, J. D. Offenberg, R. J. Hanisch, J. C. Mather, M. A. Nieto-Santisteban, R. Sengupta, and H. S. Stockman, "Cosmic-Ray Rejection and Readout Efficiency for Large-Area Arrays," *PASP* **112**, pp. 1350–1359, Oct. 2000.
19. R. G. Arendt, D. J. Fixsen, and S. H. Moseley, "Dithering Strategies for Efficient Self-Calibration of Imaging Arrays," *ApJ* **536**, pp. 500–512, June 2000.
20. C. Dragone, "A first-order treatment of aberrations in Cassegrainian and Gregorian antennas," *IEEE Transactions on Antennas and Propagation* **30**, pp. 331–339, May 1982.
21. H. Tanaka and M. Mizusawa *Inst. Electron. Commun. Eng. Japan* **58-B**, 1975.
22. S. Hanany and D. P. Marrone, "Comparison of designs of off-axis Gregorian telescopes for millimeter-wave large focal-plane arrays," *Appl. Opt.* **41**, pp. 4666–4670, Aug. 2002.
23. A. Wootten, "Atacama Large Millimeter Array (ALMA)," in *Large Ground-based Telescopes. Edited by Oschmann, Jacobus M.; Stepp, Larry M. Proceedings of the SPIE, Volume 4837, pp. 110-118 (2003).*, pp. 110–118, Feb. 2003.
24. D. Schwan, F. Bertoldi, S. Cho, M. Dobbs, R. Guesten, N. W. Halverson, W. L. Holzapfel, E. Kreysa, T. M. Lanting, A. T. Lee, M. Lueker, J. Mehl, K. Menten, D. Muders, M. Myers, T. Plagge, A. Raccanelli, P. Schilke, P. L. Richards, H. Spieler, and M. White, "APEX-SZ a Sunyaev-Zel'dovich galaxy cluster survey," *New Astronomy Review* **47**, pp. 933–937, Dec. 2003.
25. S. Padin, M. C. Shepherd, J. K. Cartwright, R. G. Keeney, B. S. Mason, T. J. Pearson, A. C. S. Readhead, W. A. Schaal, J. Sievers, P. S. Udomprasert, J. K. Yamasaki, W. L. Holzapfel, J. E. Carlstrom, M. Joy, S. T. Myers, and A. Otarola, "The Cosmic Background Imager," *PASP* **114**, pp. 83–97, Jan. 2002.
26. O. P. Lay and N. W. Halverson, "The Impact of Atmospheric Fluctuations on Degree-Scale Imaging of the Cosmic Microwave Background," *ApJ* **543**, pp. 787–798, Nov. 2000.
27. A. E. Evrard, C. A. Metzler, and J. F. Navarro, "Mass Estimates of X-Ray Clusters," *ApJ* **469**, pp. 494–+, Oct. 1996.

28. M. Arnaud and A. E. Evrard, "The L-X-T relation and intracluster gas fractions of X-ray clusters," *MNRAS* **305**, pp. 631–640, May 1999.
29. G. P. Holder, J. J. Mohr, J. E. Carlstrom, A. E. Evrard, and E. M. Leitch, "Expectations for an Interferometric Sunyaev-Zeldovich Effect Survey for Galaxy Clusters," *ApJ* **544**, pp. 629–635, Dec. 2000.